LETTER

Rapid synthesis of TiB$_2$/Fe composite in situ by spark plasma sintering

Binghong Li · Ying Liu · Hui Cao · Lin He ·
Jun Li

Introduction

Metal matrix composites (MMCs) with steel matrix and ceramic particle reinforcements are candidates for structural applications in wear-resistant materials [1–3]. Conventional production route, such as powder metallurgy (PM), often involves the addition of the reinforcing phases into the metal matrix directly, which could lead to poor wetting behavior between ceramic phase and metal matrix and segregation of reinforcements. Moreover, it is expensive and time consuming to produce MMCs by conventional PM route. Recently, in situ technique has been developed to produce ceramic particle reinforced MMCs. For the in situ technique, reinforcements are formed in situ by the chemical reaction between elements or their compounds during the fabrication process. Compared with the ex situ route, in situ process has advantages such as uniform distribution of reinforcement, finer reinforcement particle size, clear interface and thermodynamically stable reinforcement in the MMCs.

Spark plasma sintering (SPS) technique is a novel sintering process [4–8]. During the process, the heating is accomplished by spark discharges in voids between the particles, generated by an instantaneous pulsed direct current which is applied through electrodes at the top and bottom punches of the graphite die. Due to these discharges, the particle surface is activated and purified, and a self-heating phenomenon is generated between the particles, as a result of which heat transfer and mass transfer can be completed instantaneously. Therefore, SPS is capable of sintering ceramic particle reinforced composite quickly to its full

density at relatively low temperature and reduce the time available for grain growth by enhancing sintering kinetics.

Among various ceramic particulates, TiB$_2$ is expected to be one of the best reinforcements for steel matrix due to its high hardness (3400 HV), high melting point (3225 °C) and outstanding wear-resistance properties. Naturally, the TiB$_2$/Fe composite has attracted a lot of attention due to its excellent mechanical properties [9–13]. However, little work has been done on the TiB$_2$/Fe composite prepared by SPS technique. Thus, the present work is aimed at exploring the feasibility of fabricating TiB$_2$ reinforced Fe matrix composite in situ by SPS technique. It is expected that this route can provide a novel way for rapidly synthesizing TiB$_2$/Fe composite and promote its commercial application.

Experimental procedure

Commercial ferrotitanium (88.6% purity) and ferroboron (99.4% purity) were used as the starting materials. Ferrotitanium and ferroboron powders were obtained by high-energy planetary ball mill with stainless steel balls and steel vials in acetone for 2 h. Powder mixtures prepared in stoichiometric ratio corresponding to TiB$_2$ formation were undertaken by mechanical mixing in acetone for 1 h. The weight ratio of ball to powder is 3:1.

Then, the mixtures were put into a cylindrical graphite die with an inner diameter of 20 mm. The in situ reaction and densification of the milled powders were performed using the SPS system (model SPS1050, Sumitomo Coal Mining Co.). The milled powders were sintered to 800–1100 °C with a holding pressure of 30 MPa in vacuum. The applied heating rate was about 80 °C/min. During the SPS process, the temperature was monitored by a pyrometer which was focused on the surface of the die.

B. Li · Y. Liu (✉) · H. Cao · L. He · J. Li
School of Materials Science and Engineering, Sichuan University, Chengdu 610065, People's Republic of China
e-mail: Liuying5536@163.com

The relative density of the sintered specimens was determined by Archimedes' principle. The theoretical density of the corresponding composite, i.e. 6.30 g/cm^3, was simply calculated through rule of mixture [14], by considering the density values of TiB$_2$ and Fe as 4.52 and 7.87 g/cm^3, respectively. X-ray phase analysis of the specimens was performed with DX-2000 diffractometer using Cu Kα radiation operated at 30 kV and 40 mA. Microstructure investigation of the sintered composite which was prepared by metallographic procedures was done on FEI Nova NanoSEM 400 scanning electron microscope (SEM). The micro-zone composition analysis was investigated using Oxford INCA energy dispersive X-ray spectrometry (EDS) system which was attached to the SEM.

Results and discussion

Densification

The densification data and sintering behavior of the TiB$_2$/Fe composite sintered at various temperatures (900–1100 °C) with 5 min holding time are shown in Fig. 1. It can be seen that densification increases as the sintering temperature increases, reaching a maximum for the specimen sintered at 1050 °C. A maximum relative density of 98.62% can be obtained due to the activation of the plasma. The increment of the relative density is substantially in accordance with the displacement of the punch, but the displacement of the punches increases with the sintering temperature all the time. The reasons for the densification might be that with the increase of sintering temperature, the wettability between liquid phase and TiB$_2$ reinforcement is improved, which intensifies dissolution–precipitation of TiB$_2$ particles and increases the amount of liquid phase. As a result, the densification increases. However, higher sintering temperature causes severe volatilization of metal because of vacuum sintering. Furthermore, the composite is melted and overflows from the end of the mould at 1100 °C, which results in the formation of voids in the sintered specimen, thereby decreasing densification.

Phase identification

The X-ray diffraction (XRD) patterns of the starting powders and the specimen sintered at various temperatures for 5 min are shown in Fig. 2. It can be seen that the starting materials mainly consists of Fe$_2$Ti and FeB (Fig. 2a). After sintering at 1000 °C, the phases present in the specimen are α-Fe and TiB$_2$ (Fig. 2e). It indicates that the Fe$_2$Ti and FeB precursors were reduced into TiB$_2$/Fe composite.
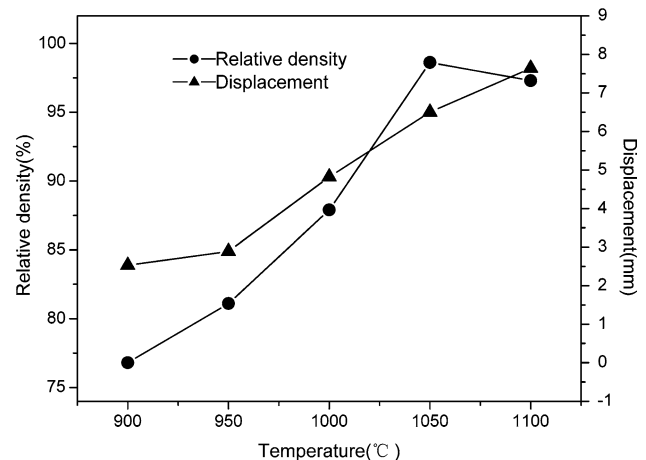

Fig. 1 Effects of sintering temperature on the relative density and displacement of TiB$_2$/Fe composite
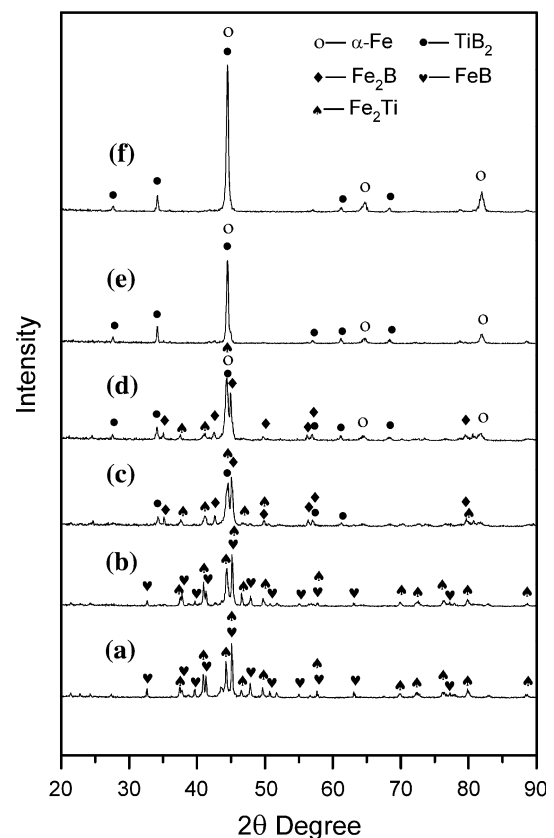
Fig. 2 XRD patterns of the specimens sintered at various temperatures: (a) starting materials, (b) 800 °C, (c) 900 °C, (d) 950 °C, (e) 1000 °C, and (f) 1050 °C

Furthermore, as shown in Fig. 2, it indicates that the in situ formation of TiB$_2$ reinforcement from ferrotitanium and ferroboron mixtures hardly occurs below 800 °C and practically completed at 1000 °C. The formation mechanism of TiB$_2$/Fe composite in situ from ferrotitanium and ferroboron may be as follows:
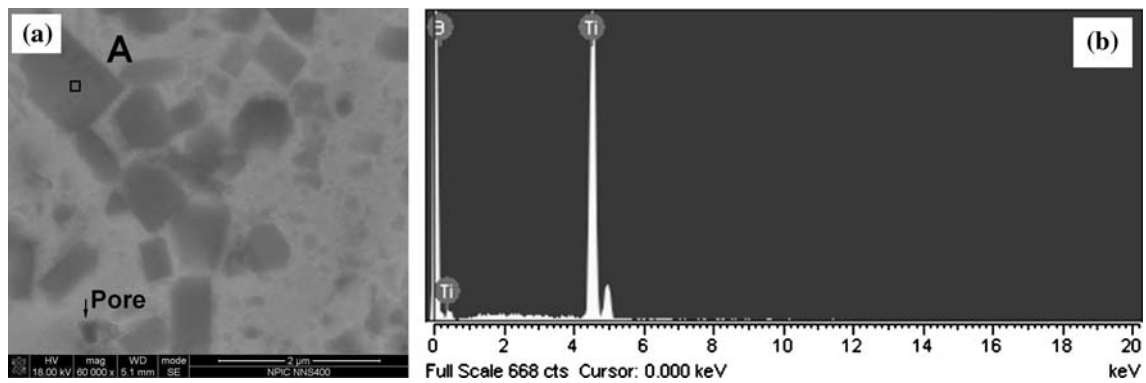
Fig. 3 EDS analysis of TiB_2/Fe composite: **a** SE micrograph and **b** EDS of point A

$$Fe_2Ti + 6FeB = 4Fe_2B + TiB_2 \qquad (1)$$

$$2Fe_2B + Fe_2Ti = 6\alpha\text{-}Fe + TiB_2 \qquad (2)$$

The first step is the solid–solid interface reaction between Fe_2Ti and FeB below 950 °C, resulting in the formation of a small amount of TiB_2 and a large amount of Fe_2B (shown in reaction (1)). The second step is the solution–precipitation in the Fe–Ti–B system at higher temperatures. The liquid phase exists at 1174 °C in Fe–Fe_2B system, but with the help of the activation of spark plasma, the liquid phase seems to appear much earlier [1, 4]. In addition, the energy from the exothermic reaction between titanium and boron may cause the temperature of the specimen in the die higher than that detected by the pyrometer [15]. When the concentration of titanium and boron in the liquids reaches supersaturation, the nucleation of TiB_2 becomes thermodynamically feasible, and then TiB_2 will be formed and precipitated out from the liquids. The hybrid formation mechanism containing solid reaction and solution–precipitation reaction were responsible for the in situ formation of TiB_2 reinforced Fe matrix composite.

Microstructure of the composite

The EDS analysis of TiB_2/Fe composite sintered at 1050 °C for 5 min is shown in Fig. 3. From the secondary electron (SE) micrograph of the specimen (Fig. 3a), it is clear that hexagonal and rectangular particulates with a size of ~ 2 μm are homogeneously distributed in the Fe matrix. The hexagonal particulates are typical TiB_2 reinforcements [11]. In addition, a few microspores can be seen in the composite. Figure 3b shows the EDS spectra of the rectangular particulates (marked by point A in Fig. 3a). Obviously, this region is rich in titanium and boron. Table 1 shows the chemical composition of the rectangular particulates. As shown in Table 1, the atomic ratio of titanium and boron is about 1:2. With the combination of the XRD results, it is evident that the rectangular

Table 1 Chemical composition of point A analyzed by EDS

Element	Weight (%)	Atomic (%)
Titanium	69.87	34.37
Boron	30.13	65.63

particulates can be identified as TiB_2. The microstructure of the TiB_2 particulates is in agreement with Ref. [16], but the size of the particulates synthesized by SPS is much smaller. It may be because that TiB_2 has not enough time to grow by the rapid SPS process, thus resulting in the fine TiB_2 particles in the matrix.

Conclusion

SPS technique has been successfully applied to the rapid synthesis of TiB_2 reinforced Fe matrix composite in situ using cheap ferrotitanium and ferroboron powders as precursors. A maximum relative density of 98.62% was obtained when the composite was sintered at 1050 °C for 5 min by the method. The in situ formation mechanism of TiB_2/Fe composite is a hybrid formation mechanism containing solid reaction and solution–precipitation reaction: first, the solid–solid interface reaction between Fe_2Ti and FeB below 950 °C, resulting in the formation of a small amount of TiB_2 and a large amount of lower melting point Fe_2B; second, the solution–precipitation reaction in the Fe–Ti–B system from 950 to 1000 °C, resulting the formation of the main TiB_2 reinforcements.

References

1. Farid A, Guo SJ, Cui FE, Feng PZ, Lin T (2007) Mater Lett 61:189
2. Farid A (2008) J Alloys Compd 459:491

3. Kumar S, Chakraborty M, Sarma VS, Murty BS (2008) Wear 265:134
4. Munir ZA, Anselmi-Tamburini U (2006) J Mater Sci 41:763. doi:10.1007/s10853-006-6555-2
5. Venkateswaran T, Basu B, Raju GB, Kim DY (2006) J Eur Ceram Soc 26:2431
6. Eriksson M, Salamon D, Nygren M, Shen ZJ (2008) Mater Sci Eng A 475:101
7. Kim JS, Kwon YS, Lomovsky OI, Korchagin MA, Mali VI, Dudina DV (2006) Mater Lett 60:3723
8. Dudina DV, Hulbert DM, Jiang DT, Unuvar C, Cytron SJ, Mukherjee AK (2008) J Mater Sci 43:3569. doi:10.1007/s10853-008-2563-8
9. Du BS, Zou ZD, Wang XH, Qu SY (2008) Appl Surf Sci 254:6489
10. Wu CF, Ma MX, Liu WJ, Zhong ML, Zhang WM, Zhang HJ (2008) Mater Lett 62:3077
11. Du BS, Zou ZD, Wang XH, Qu SY (2008) Mater Lett 62:689
12. Wang Y, Zhang ZQ, Wang HY, Ma BX, Jiang QC (2006) Mater Sci Eng A 422:339
13. Lepakova OK, Raskolenko LG, Maksimov YM (2004) J Mater Sci 39:3723. doi:10.1023/B:JMSC.0000030726.29507.2b
14. Matthews FL, Rawlings R (1994) Composite materials: engineering and science. Chapman & Hall, Uk
15. Liang YH, Wang HY, Yang YF, Du YL, Jiang QC (2008) Int J Refract Met 26:383
16. Wang HY, Huang L, Jiang QC (2005) Mater Sci Eng A 407:98